



Sustainable polyurethane nanocomposite foam from waste poly(ethylene terephthalate): preparation, thermal stability, and flame retardancy

Hai Vothi^{1,2} · VietHien Le^{1,2} · TuyetMinh Nguyen-Ha^{2,3} · DongQuy Hoang^{2,3}

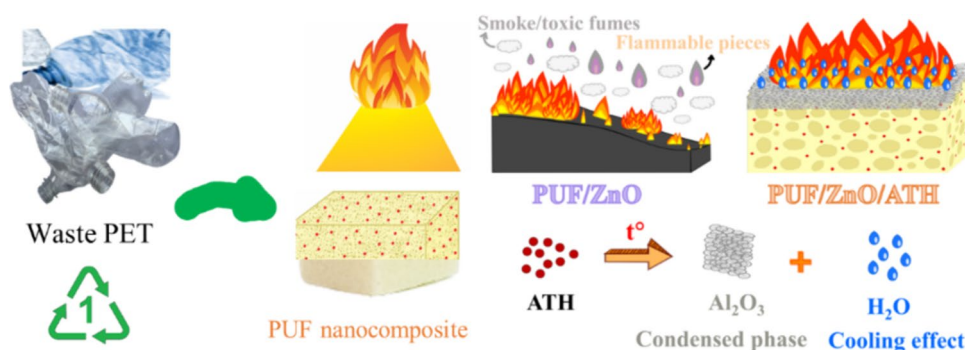
Received: 28 March 2024 / Revised: 21 July 2024 / Accepted: 22 July 2024
© The Author(s), under exclusive licence to The Polymer Society of Korea 2024

Abstract

In this work, we proposed and synthesized sustainable nanocomposite polyurethane foam (PUF) derived from waste poly(ethylene terephthalate) (PET), reinforced with nano ZnO and incorporating aluminum hydroxide (ATH) as a flame retardant. Chemical structure of oligodiols obtained from the glycolysis of waste PET by diethylene glycol and ZnSO₄·7H₂O catalyst under microwave irradiation was confirmed by FTIR and ¹H-NMR and continuously product of that was used to prepare PUF nanocomposite material. The density of the PUF decreased from 58 to 35 g/cm³ by the addition of ZnO nanoparticles, which are suitable for lightweight and insulation applications. In addition, the incorporation of ATH is indispensable to enhancing the flame retardancy of the PUF nanocomposites with UL-94 (HB) at 100 php ATH loading and UL-94 (VB) V-0 at 150 php ATH loading, simultaneously enhancing the mechanical properties of PUF/ZnO/ATH nanocomposites. The outcomes not only met the fire safety requisites, light-weight, and high mechanical properties for polymer nanocomposite material applications in construction but also incorporated a substantial proportion of discarded PET bottles sourced from associated industries.

Graphic abstract

The PUF nanocomposite foam derived from waste PET has high mechanical property and excellent flame-retardant performance to create a sustainable recycling polymer material and improve waste management.



Keywords PUF Flame retardancy · Thermal stability · Post-consumer PET · Oligodiols · Sustainable PUF nanocomposite foam · Sustainable recycling research · Aluminum trihydroxide

1 Introduction

Recently, eco-friendly fabricated process of materials from sustainable energy resources as well as the attempts in solving problems of contaminants on the earth have been

Extended author information available on the last page of the article

challenged and developed by scientists all the world. Especially, plastics have been increasingly used and it is necessary to consider life cycle of that after using. In current industrial society, polyurethane (PU) is a well-established and versatile material in today's industrial society, finding applications in the production of elastomers, adhesives, varnishes, coatings, sealants, and foams [1–5]. Especially, rigid polyurethane foam (PUF) is one kind of thermoset which is used in construction for several applications, including insulation, roofing, and wall systems [6–8]. These materials, however, arm to the major difficulties and challenges of strictly demand with important properties such as the abilities of sound performance, water resistance, and fire resistance [9, 10]. Notably, the micro-structural characteristics of PUF include cell size, foam density, and cell-size distribution affect on the final properties of PU remarkably and PUF has a high surface-to-volume ratio, and a major drawback is its high combustibility; therefore, it demands the addition of a flame retardant for processing of PUF [11].

It has been reported that metal oxide nanoparticles such as zinc oxide (ZnO) or magnesium oxide (MgO) nanoparticles (NPs), which own to their superior properties (chemical resistance, thermal stability, low toxicity, environmental friendliness, and low cost), have emerged as the most widely employed nanofillers for modifying the desired properties of PU [6, 12–14]. Furthermore, metal oxides can facilitate the formation of a substantial residual char during polymer combustion, preventing direct contact of the material with heat sources and effectively entrapping the smoke generated during combustion. This accordingly serves to shield the inner components from the combustion process [15]. Concerning the harsh environmental issues, it is necessary to apply halogen-free flame retardants (FRs) instead of the traditionally toxic and hazardous halogen-based FR [16–19]. Aluminum trihydroxide (ATH) is commonly used as an effective and outstanding filler to enhance the fire retardancy of polymer-based materials due to its cost-effectiveness and low toxicity. The flame-retardant mechanism of this inorganic filler relates to the release of water and the formation of the dense layer of Al_2O_3 during the polymer combustion, decreasing the temperature in the burning zone and protecting the inner materials from further combustion [20, 21]. Vo D. et al. reported that the combined addition of ZnO and MgO NPs not only reduces the density of PU foam but also, when used in conjunction with ATH, significantly enhances the flame retardancy of PU [22].

As a researcher, the scientists aim to focus on all of lightweight, fire resistance, and mechanical reinforcement in only one sustainable engineering PU, which is used for applying in constructions as designed and shown in Fig. 1.

PU is product from reaction of diisocyanate/polyisocyanate and diols/polyols. Polyols from commercial market such as polyether polyols, polyester polyols, and

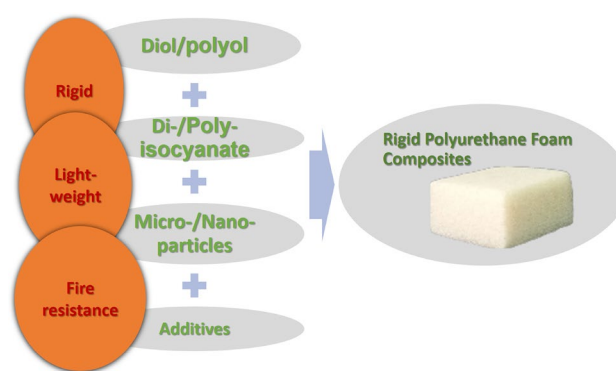


Fig. 1 Designed model of rigid polyurethane foam composite

isocyanates as methylene diphenyl diisocyanate (MDI) and toluene diisocyanate (TDI) in which MDI is the most commonly used isocyanate ingredient are one of two main ingredients to synthesize PU based on exothermic reaction between hydroxyl groups (-OH) and the isocyanate groups (-NCO) and formation of a urethane linkage (-NH-(C=O)-O-) [8, 23]. The changes in relative ratios of ingredients such as polyol, isocyanate, and additives significantly affect the final properties of the foams [24]. Polyols are traditionally derived from petrochemical feedstocks. However, a recent proposal for a more sustainable future in the industry involves the substitution of commercially available polyols with oligodiols. These oligodiols are obtained through the glycolysis of waste poly(ethylene terephthalate) (PET) and can be employed as starting materials for the synthesis of PUF [25, 26].

This study investigates the fabrication of PUF/ZnO nanocomposites with enhanced properties for lightweight material applications. To address flammability concerns, ATH is added to the PUF/ZnO nanocomposite to improve flame retardancy, a crucial property for practical insulation materials. Notably, replacement of polyol by oligodiol, which was obtained from glycolysis of waste PET and excess of diethylene glycol (DEG), was used to prepare PUF and ZnO NPs which was synthesized by the precipitation method are directly used as nano-sized fillers to fabricate PUF/ZnO nanocomposite. The addition of both NPs and ATH in PUF formulations is believed to promote the increments in mechanical, thermal, and flame-retardant performances. The density of PUF with ZnO NPs is examined, and the influence of both NPs and ATH on the physicochemical properties is evaluated using scanning electron microscopy (SEM) and compressive strength tests. In addition, the effect of ZnO NPs under present of ATH on flame-retardant behavior of PUF/ZnO/ATH nanocomposites was investigated by applying thermogravimetric analysis, vertical and horizontal UL-94 tests.

2 Experimental

2.1 Material

Zinc nitrate hexahydrate ($\text{Zn}(\text{NO}_3)_2 \cdot 6\text{H}_2\text{O}$) and aluminum hydroxide (ATH) were purchased from Xilong, China. Potassium hydroxide (KOH) were purchased from Guangdong Guanghua SciTech Co., China. Methylene diphenyl diisocyanate (MDI, Voracor CE101) was obtained from DOW Chemical, China. Dibutyltin dilaurate (DBDL) and diethylene glycol (DEG) were purchased from Merck of Germany and Sigma-Aldrich of Germany, respectively.

2.2 Synthesis of ZnO nanoparticles

ZnO NPs was synthesized from well-known method as described in previous reports [22] with some modifications. 100 mL KOH 0.4 M was slowly added dropwise into 100 mL $\text{Zn}(\text{NO}_3)_2$ 0.2 M and then the reaction mixture was continuously stirred at 800 rpm for 90 min at room temperature. The obtained white-solid precipitate was washed with distilled water, following with centrifugation in four times and dried overnight in an oven at 100 °C. Finally, the product was ground and calcined at 500 °C for 3 h to obtain the ZnO NPs. The particle size and morphology of ZnO NPs was characterized by FE-SEM with average size of particles lower than 100 nm.

2.3 Synthesis of oligodiol from waste PET

Oligodiol was synthesized based on glycolysis between waste PET and excess of DEG under microwave condition as described in literature [25]. In a 250-mL Erlenmeyer flask was added 48.0 g (0.250 mol) of PET flakes, 66.3 g (0.626 mol) of DEG (DEG/PET molar ratio = 2.5/1), and 0.427 g of $\text{ZnSO}_4 \cdot 7\text{H}_2\text{O}$ (appropriately 0.89 wt% of PET). The flask was covered with a watch glass. The household microwave oven was operated at a fixed power of 250 W and at 5 min operation intervals, followed by a 5 min pause, so that the reaction mixture would not boil. The microwave irradiation was continued until all PET flakes were completely dissolved. After the total 80 min of reaction, the mixture was cooled to room temperature and left overnight. The solid catalyst appeared at the bottom of the flask and was separated by decantation and centrifugation to obtain oligodiol which was used in the preparation of PUF on next step without further purification.

2.4 Preparation of PUF/ZnO and PUF/ZnO/ATH nanocomposites

The one-shot and free-rise techniques were used to prepare foam samples, related literature was cited on [22]. Oligodiol, water as blowing agent, silicone surfactant, and DBDL

catalyst were mixed in a metal cup for 5 min. Then, ZnO NPs and ATH were slowly added to the above mixture and stirred at 1650 rpm for 10 min to obtain a homogeneous mixture. Next, MDI was added to the cup by continuously stirring at 1000 rpm for 15 s and quickly poured into a paper mold ($7 \times 14 \times 14$ cm) and allowed to expand freely. After that, the foam was dried at 60 °C for 2 h and stabilized at room temperature for 24 h. The PUF sample without NPs was also synthesized by the same procedure. The ingredients in the synthesis process are listed in Table 1.

2.5 Measurements

Fourier-transform infrared (FT-IR) spectra were recorded using a BRUKER-IFS-66/S, TENSOR 27 spectrometer using a diamond crystal. The transition mode was used, and the wavenumber range was set as 4000–400 cm^{-1} . Proton (^1H) nuclear magnetic resonance (NMR) spectra were recorded with a Bruker ARX-500 NMR (Karlsruhe, Germany) spectrometer operating at 500 MHz and with CDCl_3 as the solvent.

The morphology and surface structure of ZnO NPs and PUF/ZnO nanocomposites was investigated using a Scanning Electron Microscopy (Hitachi Model S-4800) to operate at an accelerating voltage of 10 and 15 kV, respectively. The foam samples were sputter-coated with platinum for 120 s before scanning to provide an electrically conductive surface.

The density of the samples was measured according to ASTM D1622. The size of each sample is $50 \times 50 \times 25$ mm^3 and the average value of at least 3 samples was obtained. The compression properties of PUF nanocomposites were studied using a universal testing machine (Shimadzu—Autograph ASH-X, Japan). The sample size of $50 \times 50 \times 25$ mm^3 was compressed with a loading rate of 2.5 mm/min in the direction parallel to the foam-rising direction according to ASTM D1621.

Thermal decomposition of PUF and its nanocomposites was performed using a Thermogravimetric analysis (New Castle, DE, USA) on a Q50 Universal V4.5A TA instrument with the heating temperature range from room temperature

Table 1 Formulations of nanocomposites in this study

Ingredients	Content (php)
MDI	130, 140, 150
DBDL	0.1
Silicon oil	3.0
Water	1.0, 0.9, 0.8
ZnO NPs	1.0, 3.0, 5.0, 7.0
ATH	100, 150
php part per hundred of oligodiol by weight	

to 700 °C at a heating rate of 10 °C/min under a nitrogen atmosphere.

Flammability testing including horizontal and vertical burning was applied to evaluate the flame retardancy of PUF and its nanocomposites. Five specimens with dimensions of $127 \times 13 \times 10 \text{ mm}^3$ were tested for each sample by burning for 10 s once and twice for UL-94HB and UL-94VB, respectively. The burning rate and self-extinguishing time were recorded. Three UL-94 ratings were considered (V-0, V-1, and V-2) depending upon the average flaming time after the first/second ignitions and the occurrence of drips as shown below.

- V-0: Burning stops within 10 s and no drips allowed.
- V-1: Burning stops within 30 s and no drips allowed.
- V-2: Burning stops within 30 s and drips of flaming particles are allowed.

3 Results and discussion

3.1 Structural characterization of oligodiol product

The above-mentioned synthesized oligodiol obtained from glycolysis of waste PET in liquid state and its characterizations were determined by FT-IR and $^1\text{H-NMR}$ analysis which were presented in Fig. 2. In Fig. 2a, the presence of the $-\text{OH}$ end groups of the oligodiol were adsorbed by a broad band at wavenumbers in range of $3360\text{--}3400 \text{ cm}^{-1}$, while the ethylene ether moiety appeared as bands at 2875 cm^{-1} corresponding to the C-H symmetric stretching. Besides, vibration at 2945 cm^{-1} belongs to the C-H symmetric stretching of aromatic groups also was adsorbed, and ester groups were identified by adsorbed doublet stretching vibrations at 1065 cm^{-1} , 1123 cm^{-1} for the C-O stretching as well as C-O-H skeleton vibration at 1272 , and vibration at 1720 cm^{-1} for C=O stretching were appeared. From all these, structural characteristics of obtained oligodiol product was verified clearly and chemical structure of oligodiol was once again confirmed by $^1\text{H-NMR}$ analysis presented in Fig. 2b.

Based on chemical structure of oligodiol attached in Fig. 2, it can be clearly declared that the $^1\text{H-NMR}$ spectrum shows aromatic protons (H_a) from 7.90 to 8.15 ppm, and aliphatic CH_2 appears as multiplet signals from 3.59 to 4.51 ppm. Signal at 4.71 ppm corresponding to proton of ending hydroxyl groups (H_e). Resonance signals from 4.46 to 4.71 ppm are typical for $-\text{CH}_2\text{OCOAr}$ with an integral of almost equal to protons of ester aliphatic proton (H_b). The $^1\text{H-NMR}$ integrals are normalized with respect to one terephthalate unit or 4 aromatic protons. Resonances at 3.59 and 3.96 ppm are due to protons of the $-\text{CH}_2\text{OCH}_2-$ (ethers) (H_c) and $-\text{CH}_2\text{OH}$ (end groups) (H_d) with number of protons higher 6 times more than protons for $-\text{CH}_2\text{OCOAr}$.

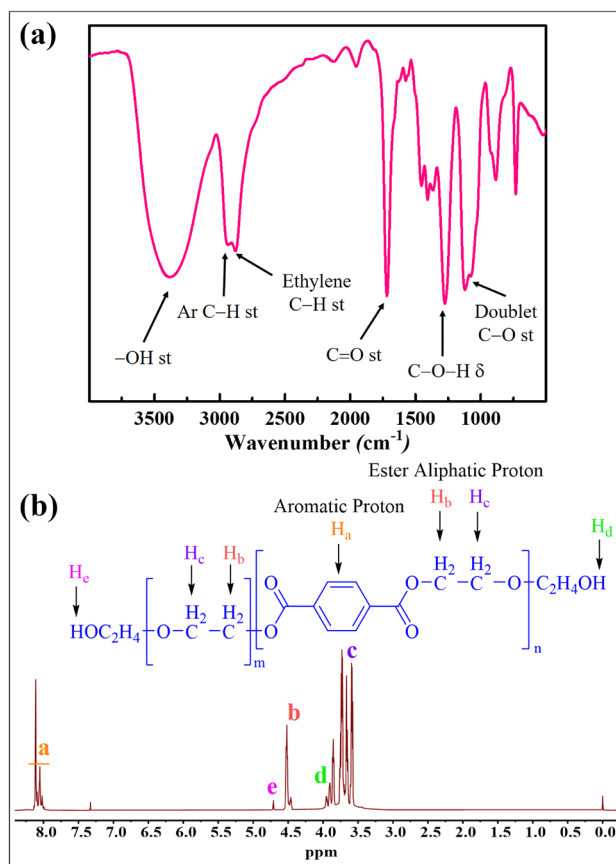


Fig. 2 a FT-IR spectra of oligodiol and b $^1\text{H-NMR}$ spectrum of oligodiol in CDCl_3

From these results, the obtained oligodiol products contains larger amount of diethylene fragments than terephthalate fragments [25].

3.2 Preparation of PUF and PUF/ZnO nanocomposites

In Table 1, the contents of MDI and water were investigated to optimize for obtaining PUF with density value as low as commercial PUF, which is the requirement for applications of lightweight structural materials. Thus, obtained PUF with MDI at 140 php and water at 0.8 php showed lowest density value at 58.0 g/cm^3 and foaming formation of cell inside has a uniform appearance, and the synthesis process with corresponding optical pictures of optimized PUF are presented in Fig. 3.

In previous published results declared that the addition of NPs leads to the appearance of nucleating agent sites which facilitating bubble formation, hence increasing the cell size in the given area and reduce the density of PU nanocomposite foams compared to neat PU foams. Therefore, in our study the effect of ZnO NPs loading amount was investigated

Fig. 3 Synthesis process, outside, and inside of PUF nanocomposite foams

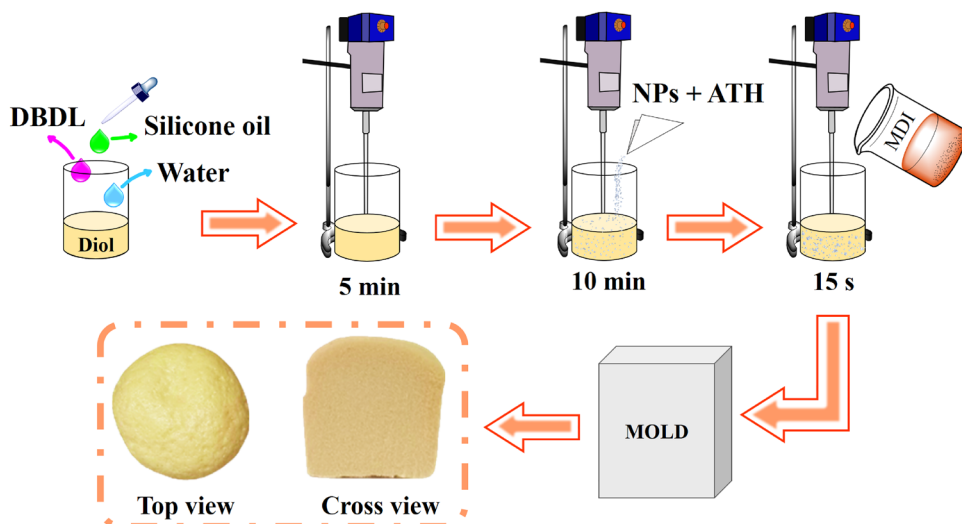







Table 2 Effect of ZnO NP loading on density of samples

Sample	Nano ZnO (php)	Picture of sample	Density (g/cm ³)
PUF	0		58.0
PUF/ZnO-1	1		40.7
PUF/ZnO-3	3		38.9
PUF/ZnO-5	5		34.9
PUF/ZnO-7	7		35.7

and not only obtained density values but also pore diameters of cells were determined in Table 2 and Fig. 4, respectively.

As shown in Table 2, increasing ZnO NPs content from 1 to 7 php showed the significant decreased density values of PUF from 58.0 to 40.7 g/cm³ of PUF/ZnO 1 php, 38.9 g/cm³ of PUF/ZnO 3 php, 34.9 g/cm³ of PUF/ZnO 5 php, 35.7 g/cm³ of PUF/ZnO 7 php, respectively. In addition, pore diameter of PUF with and without ZnO NPs were identified by SEM results presented in Fig. 4. Pore diameter of PUF is 450 ± 67 μm and that of PUF/ZnO nanocomposites at 1, 3, 5 php loading of ZnO NPs are 458 ± 89, 536 ± 77,

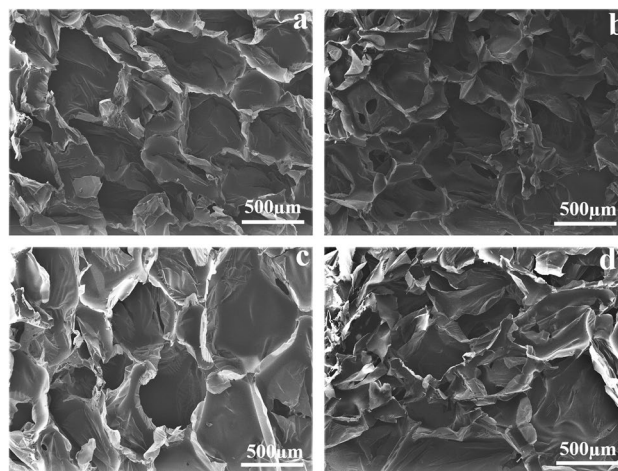


Fig. 4 SEM images of PUF (a), PUF/ZnO-1 (b), PUF/ZnO-3 (c), and PUF/ZnO-5 (d)

and 682 ± 70 μm, respectively. From these results, it can be concluded that increasing amount of ZnO NPs decreased the density values of PUF, which can be explained by increasing the pore size of cell during foaming formation. Thus, the more content of ZnO NPs, the lower density value of PUF/ZnO nanocomposite obtained.

3.3 Flame retardancy and thermal property of PUF/ZnO nanocomposites with and without ATH flame retardant

The flame retardancy of the nanocomposite foams in this study was investigated through the both horizontal and vertical burning test. It has been reported that increasing the porosity led to decrease the density of material, and thus the flammability of foam materials increases [22]. Same

obtained results in our study and the evaluated UL-94 results (HB and VB) of PUF, PUF/ZnO, and PUF/ZnO/ATH nanocomposites were shown in Table 3. From UL-94 results, both of PUF and PUF/ZnO nanocomposite specimens are burn completely due to highly flammable. It can be easily explained by the large overall surface area and high air permeability of porous materials. Therefore, ZnO nanoparticles did not improve the flammability of PUF and the adding an efficient flame retardant with low environmental hazards plays an important role to enhance their flame retardancy. Then, PUF/ZnO nanocomposite at 5 php loading of ZnO NPs was chosen for further investigation in thermal stability when applying with ATH, one of the most popular inorganic flame retardants.

To assert the above conclusion, the utilization of ATH flame retardant additive significantly increases the flammability of PUF/ZnO nanocomposites, especially with UL-94 HB obtained at 100 php loading of ATH and the flame does not reach the first 25 mm mark whilst with UL-94 VB V-0 rating obtained at 150 php loading of ATH and the flame quickly extinguishes after 5 s burning, details of that results were presented in Table 3. The addition of ATH slowed down the combustion process, leading to an increase in the fire retardancy of PU/ZnO nanocomposite materials.

In addition, a clear view of the effect of ZnO NPs and the ATH flame retardant on thermal stability of PUF were also discussed by TGA analysis which were presented in Fig. 5. In Fig. 5, all TGA curves of all samples showed two degradation steps continuously. The initial degradation temperature (Tid) of PUF was observed from 230 °C with the

release of combustible gas and adding ZnO NPs reduces slightly Tid as well as thermal stability of PUF. This result can be explained by ZnO NPs' metallic character and the polymer chains will shell the nanoparticles, reducing the number of hydrogen bonds thereby reducing the number of physical crosslinks of the PU [22]. In addition, ZnO also plays a role as a catalyst in the reaction (between -NCO free groups and -OH groups on the surface ZnO NPs) and the decomposition continues to release CO₂ and H₂O under the heating effect [27, 28], therefore, the residue of PU/ZnO

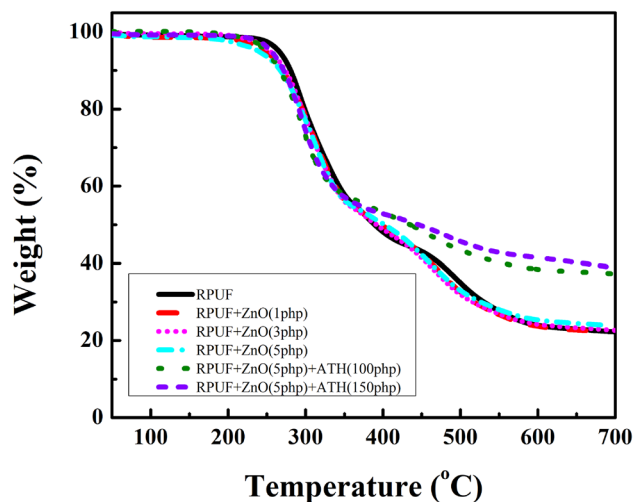









Fig. 5 TGA curves of PUF, PUF/ZnO, and PUF/ZnO/ATH nanocomposites

Table 3 UL-94 (HB and VB) results

Sample	UL-94 (HB)	Picture of sample		UL-94 (VB)	t_1/t_2 * (s/s)	Picture of sample after UL-94 (VB)
		During ignition	After UL-94 (HB)			
PUF	NR	–	Burn completely	NR	–	Burn completely
PUF/ZnO -5	NR		Burn completely	NR	–	Burn completely
PUF/ZnO-5/ATH-100	HB			V-1	11/9	
PUF/ZnO-5/ATH-150	HB			V-0	0/5	

* Time of ignition, NR no rating

nanocomposites is slightly lower than that of neat PUF after final decomposition around 450–500 °C. With the presence of ATH, the thermal stability of nanocomposites increases and the residual chars notably increase from 22.3% residue of PUF/ZnO nanocomposite to 39.0% residue of PUF/ZnO/ATH at 700 °C.

It is well-known that ATH with dehydration process through the release of water molecules, which helps to dilute the flammable gases decomposed from polyurethane matrix and lower the temperature of burning zone during combustion. In addition, the condensed Al_2O_3 phase formed during the thermal decomposition plays an important role as a protective layer, prohibiting the inner material from burning and inhibiting the toxic smoke releasing. From the above results, the possible flame-retardant mechanism of PUF/ZnO/ATH nanocomposites is exemplified in Fig. 6.

3.4 Mechanical property of PUF and PUF/ZnO nanocomposites with and without ATH

Table 4 shows the compressive strength of PUF, PUF/ZnO-1, PUF/ZnO-3, PUF/ZnO-5, PUF/ZnO-5/ATH-100, and PUF/ZnO-5/ATH-150 nanocomposites at 10% strain in this study and the results were evaluated according to ASTM D1621.

The compressive strength of PUF/ZnO-1, PUF/ZnO-3, PUF/ZnO-5 are about 35.5 ± 3.6 , 68.4 ± 17 and 65.5 ± 31 kPa, respectively, which are lower than that of PUF, about 92.7 ± 15 Kpa. Indeed, the components had an impact on the pore size of the PUF. Incorporating nano ZnO into PUF resulted in an increasing the average pore size. Furthermore, the pore size of the samples also was found to be directly correlated with their density values, as described in Table 2. The sample with a larger pore size has the lower density and compressive strength.

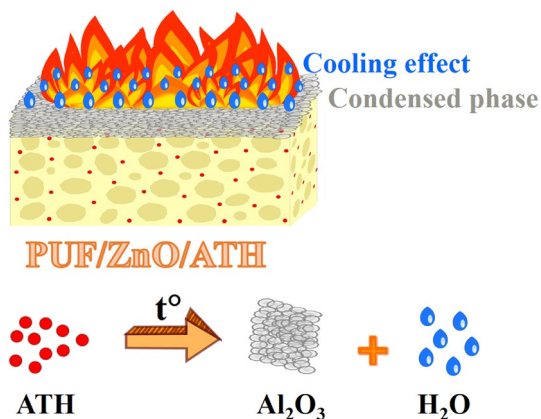


Fig. 6 Schematic of possible flame-retardant mechanism of PUF/ZnO/ATH nanocomposite

Table 4 Compressive strength of PUF/ZnO nanocomposites with and without ATH at 10% strain

Sample	Compressive strain (kPa)	Standard deviation
PUF	92.7	± 15
PUF/ZnO-1	35.5	± 3.6
PUF/ZnO-3	68.4	± 17
PUF/ZnO-5	65.5	± 31
PUF/ZnO-5/ATH-100	120.0	± 20
PUF/ZnO-5/ATH-150	93.1	± 17

Nevertheless, the samples incorporating 100 and 150 php ATH exhibit enhanced compressive strength, measuring 120.0 ± 20 and 93.1 ± 17 kPa, in contrast to 64 kPa observed in PUF/ZnO-5. The inclusion of ATH results in greater uniformity in cell size and increased thickness of cell walls, thereby enlarging the mechanical properties. On the other hand, the presence of ATH led to increasing the density of the samples (122.5 g/cm^3 for PUF/ZnO-5/ATH-100 and 153.1 g/cm^3 for PUF/ZnO-5/ATH-150) due to high bulk density of ATH. The increase in density is directly associated with the compactness of the cellular structure, which results in a higher mass per unit area. As a result, the force required for compressing the material also rises, thereby yielding increased strength. Under the effect of compressive force, ATH powders are attributed to absorb and disperse force in the PU system leading to an increase in the compressive strength of the sample. Nevertheless, ATH constitutes a metallic hydroxide utilized as a mineral filler, yet its non-reinforcing characteristic arises from its limited wetting properties. By considerable amounts (150 php ATH), the interaction of filler-filler becomes more obvious, resulting in agglomeration causing poor strength when compared to the nanocomposite sample containing 100 php ATH.

4 Conclusions

The PUF was prepared successfully by the reaction of MDI with oligodiol obtained from the glycolysis of waste PET by DEG and $\text{ZnSO}_4 \cdot 7\text{H}_2\text{O}$ catalyst under microwave irradiation. This has the potential to contribute to the reduction of recycled polymer material quantities and advancement in waste management practices.

The addition of 5 php ZnO nanoparticles into PUF matrix decreases the density of the nanocomposites compared to the pristine PUF, which are suitable for lightweight, insulation, and flame-retardant applications. In addition, the incorporation of ATH is indispensable to enhancing the flame retardancy of the PU nanocomposite foam. The ATH flame retardant enhanced the thermal stability of the PUF

nanocomposite by notably increasing the residual char content in the temperature range of 400–700 °C. This char layer acted as thermal barriers, preventing the inner layer from transferring heat and oxygen, and played an important role in the fire retardancy. The findings from this investigation also affirm that the PUF synthesized from waste PET not only satisfied the stringent requirements for fire safety and thermal stability in polymer nanocomposite applications but also comprised a substantial proportion of post-consumer PET, thus fostering the development of a sustainable recycling research.

Supplementary Information The online version contains supplementary material available at <https://doi.org/10.1007/s13233-024-00304-3>.

Acknowledgements This research is funded by Vietnam National University Ho Chi Minh City (VNU-HCM) under grant number C2022-18-44.

References

1. W.J. Lee, H.G. Oh, S.H. Cha, A brief review of self-healing polyurethane based on dynamic chemistry. *Macromol. Res.* **29**, 649–664 (2021). <https://doi.org/10.1007/s13233-021-9088-2>
2. S. Mapari, S. Mestry, S.T. Mhaske, Developments in pressure-sensitive adhesives: a review. *Polym. Bull.* **78**, 4075–4108 (2021). <https://doi.org/10.1007/s00289-020-03305-1>
3. M.R. Sanghvi, O.H. Tambare, A.P. More, Performance of various fillers in adhesives applications: a review. *Polym. Bull.* **79**, 10491–10553 (2022). <https://doi.org/10.1007/s00289-021-04022-z>
4. J. Kim, H. Jung, M. Kim et al., Conductive polymer composites for soft tactile sensors. *Macromol. Res.* **29**, 761–775 (2021). <https://doi.org/10.1007/s13233-021-9092-6>
5. R. Beran, L. Zarybnicka, D. Machova, Recycling of rigid polyurethane foam: micro-milled powder used as active filler in polyurethane adhesives. *J. Appl. Polym. Sci.* (2020). <https://doi.org/10.1002/app.49095>
6. R. Jang, Y. Lee, K.H. Song et al., Effects of nucleating agent on the thermal conductivity and creep strain behavior of rigid polyurethane foams blown by an environment-friendly foaming agent. *Macromol. Res.* **29**, 15–23 (2021). <https://doi.org/10.1007/s13233-021-9003-x>
7. I. Barszczewska-Rybarek et al., Characterization of changes in structural, physicochemical and mechanical properties of rigid polyurethane building insulation after thermal aging in air and seawater. *Polym. Bull.* **79**, 3061–3083 (2022). <https://doi.org/10.1007/s00289-021-03632-x>
8. B.S. Kim, J. Choi, Y.S. Park et al., Semi-rigid polyurethane foam and polymethylsilsesquioxane aerogel composite for thermal insulation and sound absorption. *Macromol. Res.* **30**, 245–253 (2022). <https://doi.org/10.1007/s13233-022-0026-8>
9. D.K. Chattopadhyay, D.C. Webster, Thermal stability and flame retardancy of polyurethanes. *Prog. Polym. Sci.* **34**, 1068–1133 (2009). <https://doi.org/10.1016/j.progpolymsci.2009.06.002>
10. F. Xie, T. Zhang, P. Bryant, V. Kurusinal, J.M. Colwell, B. Laycock, Degradation and stabilization of polyurethane elastomers. *Prog. Polym. Sci.* **90**, 211–268 (2019). <https://doi.org/10.1016/j.progpolymsci.2018.12.003>
11. L. Hou et al., Synergistic effect of silica aerogels and hollow glass microspheres on microstructure and thermal properties of rigid polyurethane foam. *J. Non Cryst. Solids* **592**, 121753 (2022). <https://doi.org/10.1016/j.jnoncrysol.2022.121753>
12. C. Lorusso, V. Vergaro, F. Conciauro, G. Ciccarella, P.M. Congedo, Thermal and mechanical performance of rigid polyurethane foam added with commercial nanoparticles. *Nanomater. Nanotechnol.* **7**, 184798041668411 (2017). <https://doi.org/10.1177/1847980416684117>
13. S.A. El Mogy, R.S. Youssef, A.A. Abd El Megeed, Processing of polyurethane nanocomposite reinforced with nanosized zinc oxide: effect on mechanical and acoustic properties. *Egypt. J. Chem.* (2019). <https://doi.org/10.21608/EJCHEM.2018.4655.1410>
14. M.M. Rahman, Polyurethane/Zinc oxide (pu/zno) composite—synthesis, protective property and application. *Polymers (Basel)*. **12**, 1535 (2020). <https://doi.org/10.3390/polym12071535>
15. X. Wang et al., Bio-based polyphenol tannic acid as universal linker between metal oxide nanoparticles and thermoplastic polyurethane to enhance flame retardancy and mechanical properties. *Compos. Part B Eng.* **224**, 109206 (2021). <https://doi.org/10.1016/j.compositesb.2021.109206>
16. T.R. Hull, R.J. Law, Å. Bergman, Environmental drivers for replacement of halogenated flame retardants, in *Polymer green flame retardants*. (Elsevier, Amsterdam, 2014), pp.119–179
17. N. Levința, Z. Vuluga, M. Teodorescu, M.C. Corobea, Halogen-free flame retardants for application in thermoplastics based on condensation polymers. *SN Appl. Sci.* **1**, 422 (2019). <https://doi.org/10.1007/s42452-019-0431-6>
18. H. Vahabi, F. Laoutid, M. Mehrpouya, M.R. Saeb, P. Dubois, Flame retardant polymer materials: an update and the future for 3D printing developments. *Mater. Sci. Eng. R. Rep.* **144**, 100604 (2021). <https://doi.org/10.1016/j.mser.2020.100604>
19. E. Akdogan, M. Erdem, M.E. Ureyen, M. Kaya, Rigid polyurethane foams with halogen-free flame retardants: thermal insulation, mechanical, and flame retardant properties. *J. Appl. Polym. Sci.* **137**, 47611 (2020). <https://doi.org/10.1002/app.47611>
20. S. Xu, J. Li, Q. Ye, L. Shen, H. Lin, Flame-retardant ethylene vinyl acetate composite materials by combining additions of aluminum hydroxide and melamine cyanurate: preparation and characteristic evaluations. *J. Coll. Interface Sci.* **589**, 525–531 (2021). <https://doi.org/10.1016/j.jcis.2021.01.026>
21. S. Elbasuney, Novel multi-component flame retardant system based on nanoscopic aluminium-trihydroxide (ATH). *Powder Technol.* **305**, 538–545 (2017). <https://doi.org/10.1016/j.powtec.2016.10.038>
22. D.K. Vo et al., Effect of metal oxide nanoparticles and aluminum hydroxide on the physicochemical properties and flame-retardant behavior of rigid polyurethane foam. *Constr. Build. Mater.* **356**, 129268 (2022). <https://doi.org/10.1016/j.conbuildmat.2022.129268>
23. P. E. Marcantoni and S. Gabrielli. ADDITIVES IN COMPOSITE MATERIALS : SYNTHESIS AND CHARACTERIZATION OF INNOVATIVE PROMOTERS IN POLYURETHANE BLENDS Federico Vittorio Rossi Dissertação para obtençãoGrau de Mestre em Química Orientadores : Prof Pedro Paulo de Lacerda e Oliveira Santos Dr . G. (2016).
24. Chemtura Teletech Documents. Analytical Method NCO Content Determination. 2, (2001). [Online]. Available: <http://eu.adiprene.com/corporatev2/v/index.jsp?vgnextoid=8a072522871d3310VgnVCM1000000753810aRCRD&vgnnextchannel=8a072522871d3310VgnVCM1000000753810aRCRD&vgnnextfmt=default>
25. C.N. Hoang et al., Novel Oligo-Ester-Ether-Diol prepared by waste poly(ethylene terephthalate) glycolysis and its use in preparing thermally stable and flame retardant polyurethane foam. *Polym (Basel)*. **11**, 236 (2019). <https://doi.org/10.3390/polym11020236>

26. M. Li, J. Luo, Y. Huang, X. Li, T. Yu, M. Ge, Recycling of waste poly(ethylene terephthalate) into flame-retardant rigid polyurethane foams. *J. Appl. Polym. Sci.* (2014). <https://doi.org/10.1002/app.40857>
27. S. Mohammadzadeh, M.E. Olya, A.M. Arabi, A. Shariati, M.R. Khosravi Nikou, Synthesis, characterization and application of ZnO-Ag as a nanophotocatalyst for organic compounds degradation, mechanism and economic study. *J. Environ. Sci.* **35**, 194–207 (2015). <https://doi.org/10.1016/j.jes.2015.03.030>
28. K. Nikoofar, M. Haghighi, M. Lashanizadegan, Z. Ahmadvand, ZnO nanorods: efficient and reusable catalysts for the synthesis of substituted imidazoles in water. *J. Taibah Univ. Sci.* **9**, 570–578 (2015). <https://doi.org/10.1016/j.jtusci.2014.12.007>

Authors and Affiliations

Hai Vothi^{1,2}  · VietHien Le^{1,2} · TuyetMinh Nguyen-Ha^{2,3} · DongQuy Hoang^{2,3}

✉ Hai Vothi
vthai@hcmus.edu.vn

✉ DongQuy Hoang
htdqy@hcmus.edu.vn

¹ Faculty of Chemistry, University of Science, Vietnam National University, Ho Chi Minh City 700000, Vietnam

Publisher's Note Springer Nature remains neutral with regard to jurisdictional claims in published maps and institutional affiliations.

Springer Nature or its licensor (e.g. a society or other partner) holds exclusive rights to this article under a publishing agreement with the author(s) or other rightsholder(s); author self-archiving of the accepted manuscript version of this article is solely governed by the terms of such publishing agreement and applicable law.

² Vietnam National University, Ho Chi Minh City 700000, Vietnam

³ Faculty of Materials Science and Technology, University of Science, Vietnam National University, Ho Chi Minh 700000, Vietnam